Migration as flow

Using hydrological concepts to estimate the residence time of migrating birds from the daily counts

Drever, Mark C.; Hrachowitz, Markus

DOI
10.1111/2041-210X.12727

Publication date
2017

Document Version
Accepted author manuscript

Published in
Methods in Ecology and Evolution

Citation (APA)
Drever, M. C., & Hrachowitz, M. (2017). Migration as flow: Using hydrological concepts to estimate the residence time of migrating birds from the daily counts. *Methods in Ecology and Evolution*, *8*(9), 1146–1157 . https://doi.org/10.1111/2041-210X.12727

MIGRATION AS FLOW: USING HYDROLOGICAL CONCEPTS TO ESTIMATE RESIDENCE TIME OF MIGRATING BIRDS FROM DAILY COUNTS

Mark C. Drever[1], and Markus Hrachowitz[2]

[1]Canadian Wildlife Service, Environment and Climate Change Canada, Pacific Wildlife Research Centre, 5421 Robertson Road, Delta, British Columbia, V4K 3N2, Canada. Email: mark.drever@canada.ca

[2]Water Resources Section, Faculty of Civil Engineering and Geosciences, Delft University of Technology, Stevinweg 1, 2600GA Delft, Netherlands.

Email: m.hrachowitz@tudelft.nl

Author post-print

This is the post-print version of the following article:

Drever, M., & Hrachowitz, M. (2017). Migration as flow: Using hydrological concepts to estimate residence time of migrating birds from daily counts. Methods in Ecology and Evolution, 8, 1146-1157, which has been published in final form at doi: 10.1111/2041-210X.12727.

Abstract

1. Estimating length of stay, the number of days a bird can be expected to stay at a site, at stopover sites is critical to understanding the migration ecology and estimating population sizes of birds as they move between breeding and non-breeding sites.
2. Estimating length of stay of migrating animals at stopover sites has an analogue in the hydrological concept of transit time, the amount of time that water spends in a reservoir, which can be calculated as a numerical integration of inflow and outflow rates with an underlying storage age selection function.
3. We used this approach to estimate lengths of stay of migrating Western Sandpiper (*Calidris mauri*) and Dunlin (*Calidris alpina*) based on time series of daily counts at two sites in British Columbia, Canada. The approach yielded mean transit times for Western Sandpiper during southward migration at Sidney Island that ranged between 9.6 days to 3.8 days, and showed a significant decline over time, 1992-2001, consistent with estimates from capture-mark-resight studies. Transit times during northward migration at Roberts Bank, Fraser River Delta, based on the best available information ranged from 1.8 and 3.2 days for Western Sandpiper, and had a median value of 2.0 days for Dunlin, consistent with estimates from radio-telemetry studies.
4. These results indicate that hydrological flow models may offer a means to estimate length of stay from daily counts of birds during migration. The models present an opportunity for testing alternate hypotheses regarding the roles of behavioral- versus habitat-related mechanisms driving shorebird population sizes.

Key words: stopover duration, migration ecology, shorebirds, Storage Age Selection function, residence time, transit time distribution

Introduction

Migrant birds typically stop at particular locations to rest and feed during their journeys between the breeding and non-breeding grounds. Estimating length-of-stay (LOS), the duration of time that birds stay at a stopover site, is critical to understanding the ecology and management of migratory species. As a population-level measure, the mean LOS_m is necessary information to estimate the number of birds using a particular stopover site, where the population size is typically calculated as the sum all the daily counts, or an estimate of the area under the population curve (the total number of ''bird days''), divided by LOS_m (Bishop et al. 2000, Frederiksen et al. 2001, Farmer and Durbain 2006). LOS_m will depend on the decisions made by individual birds, and can vary with time of year, distance to destination, predation risk, weather conditions, available resources, and possibly individual condition. Moreover, behavioural responses to changes in predation risk may have led to reductions in LOS_m, and could account for observed census declines of some birds (Ydenberg et al. 2004). Therefore, understanding the links between LOS and counts of birds at stopover sites may inform conservation actions for shorebird populations, many of which are in decline (Andres et al. 2012).

LOS for migratory birds is typically estimated from a sample of marked birds, using mark-recapture approaches, radio-telemetry or other tracking technology (Schaub et al. 2001). If however estimates of LOS could be derived directly from time series of count data, it would allow a historical reconstruction of past conditions, as well as a new source of information from which to evaluate behavioral decisions made by migrating birds. Further, population sizes of migrating birds as derived from counts are often used to inform schemes that prioritize conservation efforts over entire flyways (Myers et al. 1987), and therefore novel methods of estimating LOS will hold great value towards conservation of migratory bird species.

Estimation of LOS has an analogue in the hydrological concept of residence or transit time, which is a measure for the amount of time that water spends in a storage reservoir (e.g., groundwater). Transit time distributions provide a quantitative

description of how systems store and release water over time, a key requirement for successful watershed management, and in particular for pollution control. In general, the concept depicts how water volumes entering the system through precipitation will be stored in the system and released as output (e.g., stream flow) after some system specific time lags. Therefore, the system output at a given moment may only contain minor proportions of the volume that entered the system at the same time step, while most of the output is typically old water that entered the system at an earlier time. A modelling approach to estimate the distributions of time lags between corresponding inputs and outputs, i.e., the transit time distributions, requires inflow and outflow rates, as well as a mechanism that allows a plausible composition of outflows from the varying water volumes of different age stored in the system at any time are required (see Methods section; e.g. Rinaldo et al., 2015).

Extending this hydrological analogy to bird migration, a count of birds at a stopover site can be considered as the storage volume at that moment, which rises and falls in an observable way over the migration period (Figs. 1-3a). The numbers of birds arriving at or leaving that stopover site at a given time then correspond to inflow or outflow rates, although these rates are often problematic to observe and thus frequently unavailable. However, when counts are made at consecutive time steps (e.g., days), the difference between two successive counts is a measure of the net flow of birds over that period (Figs. 1-3b), which may serve to provide reasonable bounds for outflow and inflow rates. Using a minimum set of assumptions, along with simplified but plausible migration mechanisms, it may be possible to infer transit time distributions with an inverse modelling approach.

In this paper, we used bird count data for two shorebird species stopping over in British Columbia, Canada, as the system state values from which we derived estimates for input and output to the system for each time step. We then used these data to construct a model that related the distributions of residence times and transit times of birds through the hydrological concept of a storage selection function. Adopting an inverse modelling strategy, we tested a high number of possible parameter

combinations for the storage selection function to analyse which combinations could result in realistic LOS values, based on existing studies based on individually-marked birds. Using this restricted set of models, we derived transit time distributions and mean transit times, and tested whether we could detect trends over time. The overall intent of the paper was to provide a proof of concept of the suggested approach, together with a review of the assumptions and limitations involved as well as an outline of its future potential.

Materials and Methods

Estimates of Length of Stay and Field Counts

LOS estimates are typically based on a sample of marked birds, using mark-recapture approaches, radio-telemetry or other tracking technology, although such estimates can be biased (Schaub et al. 2001). Observations of marked birds allow the calculation of LOS as the duration of time that the sample of n=1,…,N individual birds spend at a stop-over site, such that:

(1)

$$LOS_n = t_R = t_{o,n} - t_{i,n}$$

where $t_{i,n}$ is the day the n^{th} individual bird is first seen at the observation site and $t_{o,n}$ is the day the same bird is last seen at the site. At any time t, these counts provide a distribution of LOS for the birds leaving the stopover site at that time:

(2)

$$p_{LOS}(t_R, t) = \frac{n(t_R, t)}{n(t)}$$

where $n(t_R,t)$ is the number of birds with a length of stay t_R that are leaving the site at a given time *t*, and $n(t)$ is the total number of birds present at that time *t*. Typically the mean LOS_m over a specified period is used to characterize migration patterns (e.g., Ydenberg et al., 2004; Hope et al., 2011). It is inferred from the marginal distribution $p_{LOS}(t_R)$ over that time period.

In this study, we used daily counts of unmarked birds and estimates of LOS estimates from marked birds available from two stopover sites. The first site, Sidney

Island (48°37’39’N, 123°19’30”W), lies 4km off the coast of Vancouver Island in southwestern British Columbia. Western Sandpipers (*Calidris mauri*) stopover during southward migration within a 96-ha lagoon located in the Gulf Islands National Park Reserve. Adult birds migrate through in July, and juvenile birds following in August and September (Butler et al. 1987). Daily counts were conducted from 1992 to 2001, beginning in early July and ending in early September of each year. Counts were made with binoculars, or with a spotting scope, depending on the proximity of the birds. This site was the location of a capture-mark-resight (CMR) study using individually-marked Western Sandpipers from 1992 to 2001, from which we obtained 10 annual estimates of mean LOS_m (Ydenberg et al. 2004).

The second site, Roberts Bank (49° 3.5'N, 123° 9.8'W), is a large mudflat (8 km^2) situated within the Fraser River Delta, British Columbia. Regular surveys of Western Sandpiper and Dunlin (*Calidris alpina*) have been conducted during northward migration at Roberts Bank between April and May since 1991 to 2015 (Drever et al. 2014). Estimates of LOS_m on the Fraser River Delta were available from a few studies of radio-marked birds conducted on the Pacific Flyway (Iverson et al. 1996, Warnock and Bishop 1998, Warnock et al. 2004, Warnock et al. 2006), from which we derived 4 estimates of LOS_m for Western Sandpipers and 1 estimate for Dunlin.

Estimating residence and transit times

Definitions and Concepts

Many natural systems allow for temporal storage of input fluxes before they are gradually released from the system as output. The way these systems store and release these inputs is a fundamental descriptor of their internal functioning (Rinaldo et al., 2015). Integrated stochastic descriptors provide robust representations of system response dynamics, and have a long history of applications in hydrology, where frequently only observations at the catchment outlet are available (McGuire and McDonnell, 2006; Birkel and Soulsby, 2015; Hrachowitz et al., 2016).

Conceptually, such systems can be represented by one or more storage components (e.g., groundwater in hydrology; stopover site in migration studies), and here we review the basic principles – symbols, descriptions and their dimensional units are presented in Table 1. Input fluxes J (i.e., precipitation per time step in hydrology; number of arriving birds per time step) enter the storage at different points in time t_i. Considering the case of no output O from the system, the storage volume S(t) at any time t (e.g., water volume stored in groundwater storage; number of birds at stopover site) then consists of the individual volumes $S(t_R,t)$ of different age (or residence time) $t_R = t - t_i$ (for $t > t_i$) that entered the system as inputs $J(t_i)$ in the past. Normalizing the storage volumes of different age by the total storage volume then gives the distribution of different ages in storage at time t, namely the residence time distribution $p_R(t_R,t) = S(t_R,t)/S(t)$. If there are no further inputs to and outputs from the system, the stored volume, and thus p_R, only experiences aging. In other words, the change of residence time t_R of all stored particles equals the change in time t, which can be expressed as (Benettin et al., 2013):

(3)

$$\frac{\partial}{\partial t}[S(t)p_R(t_R,t)] + \frac{\partial}{\partial t_r}[S(t)p_R(t_R,t)] = 0$$

Where inputs J(t) to the system are equivalent to the proportion of the storage volume S(t) with age zero and define the boundary condition:

(4)

$$p_R(0,t) = J(t)/S(t)$$

Thus, with additional inputs $J(t_i)$ and outputs O(t) and considering that O(t) can only be composed of a sample from what is stored as S(t) (Fig.4), equation (3) can, under conservation of mass dS/dt=J(t)-O(t), be expanded and rearranged to provide the Master Equation of residence time distributions p_R as formulated by Botter et al. (2011):

(5)

$$\frac{\partial p_R(t_R,t)}{\partial t} + \frac{\partial p_R(t_R,t)}{\partial t_R} = -p_R(t_R,t)\frac{J(t)-O(t)}{S(t)} - \frac{O(t)}{S(t)}p_T(t_R,t)$$

Where $p_T(t_R,t)$ is the transit time distribution, i.e., the age distribution of the output O(t). As the output at any time t can only be a sample of the residence time distribution $p_R(t_R,t)$, it can be readily expressed as a function thereof (Botter et al., 2011):

(6)

$$p_T(t_R,t) = p_R(t_R,t)\omega(t_R,t)$$

Where ω is a function, typically referred to as Storage Age Selection (SAS) function (Rinaldo et al., 2015), determining how the contents with different residence times stored in the system are sampled to form the output O(t). The function's shape depends on how the system samples from the resident storage. For example, a random sampling scheme, i.e. $\omega(t_R,t)=1$, samples the stored ages in the same proportion as they are stored in the system (Benettin et al., 2013), not giving any preference to younger or older ages (Fig.4a). Alternatively, SAS functions with low modes allow for preferably sampling from younger resident ages (Fig.4b), and functions with higher modes allow for preferable sampling of older ages (Fig.4c; Botter, 2012; Van der Velde et al., 2012). Equation (6) further illustrates that p_R and p_T are strictly only equivalent in the case of random sampling. Note that to conserve mass, ω always needs to satisfy (Harman, 2015):

(7)

$$\int_0^\infty p_T(t_R,t)dt_R = \int_0^\infty p_R(t_R,t)\omega(t_R,t)dt_R = 1$$

Equation (5) implies that in non-stationary systems, characterized by variable flow, the residence time distribution p_R is intrinsically variable in time as a result of the history of input and output fluxes in the past (Botter et al., 2011). From equation (7) thus follows that ω is dependent on p_R. Therefore, closed form parameterizations of ω are only available for random sampling and similarly simple cases (Harman 2015). Transformed expressions of ω need to be used otherwise. A convenient approach is to use the cumulative residence time distribution $P_R(t_R,t)$ as a transformed domain for ω, bounding it to the interval [0,1]:

(8)

$$\int_0^1 \omega(P_R, t) dP_R = 1$$

Such transformed SAS functions can then also be defined as temporally variable expressions (e.g. Hrachowitz et al., 2013) if required by a system that is evolving over time (e.g. Brooks et al., 2010) and warranted by the data available.

The difference between p_R and p_T can be illustrated by their analogy to population models (Benettin et al., 2015a; Hrachowitz et al., 2016). The residence time distribution p_R is analogous to the distribution of ages of all individuals of a population born in the past and still alive at a given moment. In contrast, the transit time distribution p_T is equivalent to the age distribution of individuals born in the past and passing away at a given moment, i.e. the age distribution at death. From the above equations and definitions follows that LOS estimates in bird migration studies, computed by equations (1), as well as the associated distributions and moments as defined by equation (2), are the conceptual equivalent of transit times and their distributions $p_T(t_R,t)$.

For further details and examples of applications of the concept in hydrology the reader is referred to recent literature on the topic (e.g. Botter et al., 2010; Rinaldo et al., 2011; Birkel et al., 2014; Benettin et al., 2015b; Harman, 2015; Hrachowitz et al., 2015; Soulsby et al., 2015).

Model implementation

Here only the state of the system, i.e. the storage (count of birds at the stopover sites) at any time t is known. From a time series of daily counts, the net flow, i.e. storage change, between two time steps t, given as:

(9)

$$\frac{dS}{dt} = S(t) - S(t + \Delta t) = J(t) - O(t)$$

can be inferred under the assumptions of conservation of mass, i.e. 100% bird survival rate over the stopover period, and a negligible number of birds returning to the site once they leave the area. Note that equation (9) allows for input and output rates to vary with time, but holds no further information about the actual values of J(t) and O(t),

which are however required to obtain estimates of p_R and p_T, as illustrated by equation (5).

This lack of information was here approached by Monte Carlo sampling with $k=10^6$ model realizations. As a first step it had to be acknowledged that the bird counts may be subject to uncertainty. An error of 25% around the daily counts was assumed, based on several comparisons of field counts and more reliable counts (Rappoldt et al., 1985), including comparisons done at the Roberts Bank site (Drever et al., 2014). For each time step and each model realization, the bird count S(t) at the stopover site was therefore then randomly sampled from the observed value ±25% (Figs.1-3a). The resulting S(t) series over the observation period then served as a basis for estimates of J(t) and O(t) for each model realization. Under the assumption that birds arriving at each time step do not leave the stopover site during the same time step, the change of the number of individual birds present at the site dS/dt defines the upper and lower bounds of possible inflow J(t) and outflow O(t) rates for each time step in each model realization:

(10)

$$J_{min}(t) < J(t) \leq J_{max}(t)$$

(11)

$$O_{min}(t) < O(t) \leq O_{max}(t)$$

Where

(12)

$$J_{min}(t) = \begin{cases} S(t+\Delta t) - S(t), & for\ S(t) < S(t+\Delta t) \\ 0, & for\ S(t) \geq S(t+\Delta t) \end{cases}$$

(13)

$$J_{max}(t) = S(t+\Delta t)$$

(14)

$$O_{min}(t) = \begin{cases} 0, & for\ S(t) < S(t+\Delta t) \\ S(t) - S(t+\Delta t), & for\ S(t) \geq S(t+\Delta t) \end{cases}$$

(15)

$$O_{max}(t) = S(t + \Delta t)$$

Following equations (10) and (11), J(t) and O(t) were randomly sampled between their respective upper and lower bounds at each time step for each model realization. The 10^6 realizations of sampled time series of J(t) (Figs. 1-3b) and O(t) (Figs. 1-3c) were then used to estimate plausible ranges of transit time distributions p_T for each observation year according to equation (7).

The relationship between birds entering and leaving the site is controlled by the storage age function ω which defines how long individual birds remain at a stopover site and the pattern to which they leave again, both of which are *a priori* unknown. To account for this lack of knowledge, the beta distribution was selected as the SAS function for its flexibility in representing distinct shapes:

(16)

$$\omega(t_R) = \frac{{t_R}^{\propto-1}(1 - t_R)^{\beta-1}}{B(\alpha, \beta)}$$

where B is the beta function and α and β are shape parameters. For each of the 10^6 model realizations α and β were sampled from uniform prior distributions with lower and upper bounds of 0.0001 and 10, respectively. The beta function allowed a wide spectrum of possible shapes for the SAS functions, including no storage age preference (α=1, β=1; Fig. 4a), preference for younger ages (α<1, β>1; Fig.4b), and preference for older ages (α>1, β<1; Fig.4c).

Following the above resulted in a conditional distribution of ages of the birds leaving the stopover site, i.e., $p_T(t_R,t)$, for each time step of each model realization. The mean transit times $p_{T,m}$ were then computed from the marginal distributions $p_T(t_R)$ of each year, i.e. the flow-weighted mean of the conditional distributions $p_T(t_R,t)$. We then compared the modelled $p_{T,m}$ to LOS_m estimates from observations to identify feasible parameter ranges for α and β for each year with available observations. More specifically, for the λ=1,..,Λ years with available CMR or radio-telemetry based benchmark LOS_m estimates the model realizations that resulted in $p_{T,m}$ within ±25% of LOS_m were retained as feasible. An informal likelihood weight, was then used to

construct uncertainty intervals for α, β, ω and p_T and to estimate a plausible range of $p_{T,m}$ given LOS_m (e.g. Freer et al., 1996):

(17)

$$L(\propto_{k,\lambda}, \beta_{k,\lambda} | LOS_{m,\lambda}) = \left(1 - \frac{|LOS_{m,\lambda} - p_{T,m,k}|}{LOS_{m,\lambda}}\right)^p$$

Where $L(\alpha_{k,\lambda},\beta_{k,\lambda}|LOS_{m,\lambda})$ is the likelihood measure for α and β of the k^{th} model realization in the λ^{th} year given the benchmark $LOS_{m,\lambda}$ and $p_{T,m,k,\lambda}$ is the mean transit time of the k^{th} model realization in the λ^{th} year.

To evaluate the models' potential for predicting $p_{T,m}$, a leave-one-out-cross-validation analysis was performed (Shao, 1993). Briefly, the posterior parameter distributions of α and β obtained from equation (17) for each year λ were, in turn, used to predict $p_{T,m}$ for the remaining Λ-1 years by running 10^5 Monte Carlo realizations, sampling α and β from the posterior distribution associated with the λ^{th} year. The predictions were then assessed based on the absolute errors to LOS_m. For Roberts Bank, counts of birds were available for a number of years when no LOS_m estimates were available. For these years, $p_{T,m}$ was predicted by sampling from the combined posterior distributions of α and β obtained from the Λ years with available LOS_m. The models in this study were implemented in MATLAB R2013b.

Results

Sidney Island. The flow dynamics of Western Sandpipers during southern migration at Sidney Island were characterized by robust estimates for ω functions across the study period. The β parameters for individual years had narrow feasible ranges, as illustrated by the $5/95^{th}$ interquantile range ($IQR_{5/95}$) of their posterior distributions (Fig.1d): the observed migration patterns can only be reproduced with $\beta << 1$. These parameter values indicate that, of the birds present at the stopover site at a given time, the ones most likely to leave are the ones that had arrived the longest time ago, while all others tend to remain at the site. The β values increased between 1992 and 2001, resulting in a gradual shift towards a less pronounced preference for old ages (Fig.1d).

This shift translates into changes in the transit time distributions p_T over time (Figs.1e,5a). The results suggest that in 1992, some birds remained at the site for more than 20 days, and that by 2001, all birds have left the site after ~9 days.

The associated estimates of overall mean transit times $p_{T,m}$ derived from the likelihood weighted combination of all k model realizations for each year reflects a similar picture with a significant decrease over time (a=-0.56±0.13, b=1127±271, R^2=0.74, p=0.007) from 9.6 days ($IQR_{5/95}$=8.2-10.7 days) in 1992 to 3.8 days in 2001 ($IQR_{5/95}$=3.3-4.3 days; inset Fig.5a). Both the solution that provided the best match to the benchmark LOS_m and the likelihood weighted overall $p_{T,m}$ of all feasible solutions very closely reproduced LOS_m and its change over each year (Fig.5a). Cross validation analysis suggests that, due to the well-defined ω at this site, the method held good predictive power, as illustrated by the low overall median absolute cross validation error of about 1 day (Fig.6a). It can, however, also be seen that $p_{T,m}$ for the year 1992, which was characterized by a markedly different migration pattern than the other years, was less well predicted (median cross validation error -4.5 days) based on information available from the other years.

Roberts Bank. The model results for Western Sandpipers at Roberts Bank, where only 4 years of LOS_m estimates were available from existing studies, showed different features. No well-defined shape of ω emerged as the most suitable for describing migration pattern at this site (Fig.2d). The ω-function shapes giving preference to old ages (dark shaded areas in Fig.2d) provided $p_{T,m}$ estimates that best matched the benchmark LOS_m, although other types of shapes also provided similarly feasible results. This uncertainty was also reflected in the largely uninformative posterior parameter distributions ($\alpha_{5/95}$=0.9-9.1, $\beta_{5/95}$=0.001-8.3).

The p_T of the 4 years exhibit a high degree of similarity, with the exception of 1992 (Fig.2e), and suggest that stopover durations were relatively short, with very few birds remaining at the site for longer than one week (Figs.2e,5b). The resulting median $p_{T,m}$ of all likelihood weighted feasible solutions ranged between 3.2 days ($IQR_{5/95}$=2.7-3.6; inset

Fig.5b) in 1992 and 1.8 days ($IQR_{5/95}$=1.5-1.8) in 2002, which are close to LOS_m (Iverson et al. 1996; Warnock and Bishop 1998; Warnock et al. 2004; Warnock et al. 2006).

The overall median $p_{T,m}$ cross validation error of about -0.6 days (Fig.6b) indicates that the model provided robust, yet negatively biased predictions, of $p_{T,m}$. The p_T (Fig.2e, 5b) and the $p_{T,m}$ (inset Fig.5b) were predicted for the years without LOS_m estimates based on relatively uninformative prior distributions of α and β (and thus ω), reflecting the combined posterior distributions of the benchmark years (Fig.2d). Given the limited knowledge on the shape of ω and the similar observed storage patterns in these years, the predicted $p_{T,m}$ estimates remain rather stable over the years with a median value of 1.8 days and no significant temporal trend (a=0.007±0.004, b=-11.4±8.4, R^2=0.12, p=0.14). The year 1998 was an exception, as the pattern of observed counts was markedly distinct to other years (Fig.2a), resulting in distinct p_T (Fig.2e,5b) and a low $p_{T,m}$ of 1.2 days ($IQR_{5/95}$=1.1-1.3 days).

Similar results were obtained for the migration dynamics of Dunlin (Fig.3e). The modelled $p_{T,m}$ for the year 2001 showed a median value of 2.0 days ($IQR_{5/95}$=1.7-2.2 days; inset Fig.5c), reproducing closely the LOS_m of 2.2 days for that year (Fig.5c). The model provided a robust result in spite of poorly identifiable parameters α and β ($\alpha_{5/95}$=0.7-9.2, $\beta_{5/95}$=0.002-9.1; Fig.3d). Thus, similar to Western Sandpiper at the Roberts Bank, roughly equivalent estimates of $p_{T,m}$ could be obtained irrespective of the shape of ω used. The p_T and $p_{T,m}$ predicted for the remaining years, on basis of the posterior distribution of α and β (and thus ω; Fig.3d) for 2001, showed little variability (Fig.3e,5c) and provided a median $p_{T,m}$ of 1.7 days. No temporal trend in $p_{T,m}$ could be detected (a=0.005±0.003, b=-7.4±6.3, R^2=0.09, p=0.17). Only the year 1998 exhibited different migration dynamics (Fig.3a), resulting in a lower $p_{T,m}$ of 1.3 days ($IQR_{5/95}$=1.1-1.4 days).

Discussion

Treating migration as a flow process, and estimating mean transit times of shorebird populations at stopover sites based on the hydrological concept of SAS

functions exhibits considerable potential to describe migration patterns. Estimates of $p_{T,m}$ obtained here were comparable to values of LOS_m derived from field studies of marked or radio-tagged birds at two sites in British Columbia. This congruence indicates that available daily counts of unmarked birds may hold sufficient information to estimate population-level LOS_m. This approach adds to a developing body of theory describing avian migration as a physical process of flow (e.g., Iwamura et al. 2013, Taylor et al. 2016), and should be applicable to any situation where daily counts of migratory species are made at stopover sites. Importantly, the approach does assume that animals flow through only once, and thus will not be useful for sites where large proportions of the population can be expected to return to the site during the migration period. Similarly, this approach assumes 100% survival over the migration period at the site, as it not possible to distinguish between emigration and death from count data alone. The assumption may introduce a slight downward bias on mean transit estimates. However, given the absence of a significant number of dead bird bodies found at the stopover sites, mortality rates at the stopover sites can be considered very minor. Further, this approach assumes that birds do not enter and depart in the same time interval, i.e., in the same day. This is a limitation introduced by the survey design, where counts are done only once per day due to the need to standardize the tide height, but does not significantly influence the results here. In the extreme and theoretical case of birds leaving again right after arrival, the lower bounds of $p_{T,m}$ would decrease from 1 day to 0 days (Fig.5). However, note that assumption can potentially introduce a stronger bias if observations were available only at coarser temporal resolutions (e.g. weekly).

Estimates of mean transit time were improved when restricting the range of possible solutions by using existing information of LOS. In the absence of any information on LOS and when only bird counts are available, the method allows, at the very least, to quantify the lower and upper limits of physically possible $p_{T,m}$. In that case, the lower physical limit of $p_{T,m}$ is 1 day. This limit follows from the hypothetical situation in which all the birds present at the site at t leave at t, i.e. $O(t)=O_{max}(t)$ (equations 10-15). The upper bounds on $p_{T,m}$ are controlled by the choice of ω. In the absence of more

detailed information on the SAS function, a beta distribution with conservative, uninformative prior parameter distributions covers a wide range of functional shapes (see above). From the set of theoretically possible shapes, the one converging towards a maximum $p_{T,m}$ can be computationally estimated with simple Monte Carlo sampling. The upper bounds on $p_{T,m}$ also depend on the pattern of changes in S, or bird counts, during the migration period. A smooth time series of S (i.e., a high average lag-1 autocorrelation coefficient) indicates higher upper bounds for $p_{T,m}$, whereas a more spiky signal (i.e., low lag-1 autocorrelation) translates into shorter upper bounds. As a thought experiment, consider a number of n birds arriving at a site at the beginning of the migration period. If no further birds arrive, and if S=n is maintained until the end of the migration period T, all birds present at the site are required to stay until T and only then leave again. This pattern translates into the longest possible mean transit time $p_{T,m}$=T. Conversely, if the series of S is a recurring sequence of n=S birds arriving at t and a subsequent reduction to S=0 at t+Δt, this pattern indicates that the maximum $p_{T,m}$=1, in which case the upper and lower bounds collapse to the same value as $O(t)=O_{max}(t)$.

As illustrated in the insets of Fig.5a-c, even if only daily bird counts S and no further information on the population-level migration dynamics are available, the above considerations can be used to distinguish migration patterns of different populations. For the Western Sandpiper at Sidney Island, upper bounds of $p_{T,m}$ ranged between 5-12 days and reflected the decrease of $p_{T,m}$ over the observation period (inset Fig.5a), attributed to increased predation risk at the site (Ydenberg et al. 2004). The populations at Roberts Bank, in contrast, showed upper bounds of $p_{T,m}$ approximately 4 to 6 days (insets Fig.5b and Fig.5c), reflecting lower LOS_m at this site. The relatively wide interval between upper and lower bounds of $p_{T,m}$ at low absolute values does, however, conceal potential temporal trends in $p_{T,m}$ at Roberts Bank.

If LOS_m estimates are available for a few years, they have the potential to hold some informative value to allow predictions of $p_{T,m}$ (based on estimates of S) in years when no LOS_m estimates are available, depending on how well ω and its temporal variation is identified in the individual years with available LOS_m. With well-defined ω, robust

predictions may detect inter-annual variations in $p_{T,m}$. For example, using the well-defined ω (Fig.1d) at Sidney island, obtained from 7 years, the $p_{T,m}$ of the remaining 8^{th} year could be predicted within approximately -1 day on average. In spite of the higher cross validation errors for the years with the longest $p_{T,m}$ (1992-1994), a certain, albeit attenuated, temporal trend in $p_{T,m}$ over the years could also be maintained (inset Fig.6a).

At Roberts Bank, where ω for both species remained less well defined (Figs.2d,3d), the predictions nevertheless resulted in low cross validation errors approximately -0.6 days (Fig.6b). Therefore, limited additional information in the posterior parameter distributions has the potential to provide robust, albeit slightly negatively biased, predictions of $p_{T,m}$ within constrained bounds. Temporal variations, however, are very likely to remain undetected in this case (Figs. 5b,c) and more information would be necessary to obtain more accurate estimates of $p_{T,m}$.

Additional information to meaningfully constrain ω and thus $p_{T,m}$ includes anecdotal observations of inflow or outflow rates for one or more time steps during a migration period, e.g., with correlations with daily weather conditions. Likewise, qualitative understanding of the social and physiological components of migration could help to understand how and if early and late arriving birds mix to leave a stopover site again. This information could provide an efficient constraint on ω. For example, the well-defined ω with strong preferences for old ages at Sidney Island implies that essentially all birds remain at the site for a minimum of time, and that the individuals in the groups of birds arriving together will also leave together without significant mixing of individuals between the groups arriving at different times. Furthermore, it is conceivable that ω may change over time due to a range of reasons such as predation risk, climate/weather conditions and food availability (Butler et al. 1997, Ydenberg et al. 2004). Any understanding of the influences of such processes could in principle be readily included in the presented modelling approach and be expected to add constraining power to ω and thus to the estimates of $p_{T,m}$.

In summary, we used time series of daily counts of shorebirds to estimate upper and lower bounds on daily net flow of birds into and out of two stopover sites, and integrated these flow estimates in a modelling approach based on the hydrological concept of SAS functions. This approach yielded robust descriptions of transit time distributions and the associated $p_{T,m}$ for shorebirds, consistent with previous studies of individually-marked birds. The method bears considerable potential to predict at least the upper and lower bounds of $p_{T,m}$ based on daily counts, with more precise predictions if more information on migration patterns becomes available. The results further indicate that, in the absence of other information about LOS, SAS-based flow models may offer a means to estimate population sizes of shorebirds at stopover sites when daily counts are available. These models thus present an opportunity for testing alternate hypotheses regarding the roles of behavioral- versus habitat-related factors that influence shorebird populations over a flyway.

Acknowledgements

We thank all the people involved in collecting the field data, including Christopher Schmidt, Rob Butler, Colin French, Holly Middleton, Terry Sullivan, Jan Ferrigan, Christopher Guglielmo, Stephanie Hazlitt, Darren Lissimore, Andrea Pomeroy, Dana Seaman, Silke Nebel, Moira Lemon, and Dan Shervill. Permission to work on Sidney Island was granted by BC Parks and Parks Canada, and by the Corporation of Delta for Roberts Bank. Barry Smith and David Hope provided estimates of LOS derived from the capture studies at Sidney Island, and Nils Warnock provided estimates from radio-telemetry studies on the Pacific coast. This work was made possible with support from the Canadian Wildlife Service of Environment and Climate Change Canada.

Data accessibility

All datasets used in this paper will be available on the Open Data Portal of the Government of Canada, or available directly through contacting the authors. The model code (MATLAB R2013b) can be made available on request.

Author Contributions

MCD and MH conceived the ideas; MD collected and collated the data; MH designed methodology and analysed the data; MCD and MH led the writing of the manuscript. All authors contributed critically to the drafts and gave final approval for publication.

References

Andres, B. A., Smith, P. A., Morrison, R. G., Gratto-Trevor, C. L., Brown, S. C., & Friis, C. A. (2012). Population estimates of North American shorebirds, 2012. Wader Study Group Bulletin 119, 178-194.

Benettin, P., Velde, Y., Zee, S. E., Rinaldo, A., & Botter, G. (2013). Chloride circulation in a lowland catchment and the formulation of transport by travel time distributions. Water Resources Research, 49(8), 4619-4632.

Benettin, P., Rinaldo, A., & Botter, G. (2015a). Tracking residence times in hydrological systems: forward and backward formulations. Hydrological Processes 29(25), 5203-5213.

Benettin, P., Kirchner, J. W., Rinaldo, A., & Botter, G. (2015b). Modeling chloride transport using travel time distributions at Plynlimon, Wales. Water Resources Research 51(5), 3259-3276.

Birkel, C., Soulsby, C., & Tetzlaff, D. (2014). Developing a consistent process-based conceptualization of catchment functioning using measurements of internal state variables. Water Resources Research, 50(4), 3481-3501.

Birkel, C., & Soulsby, C. (2015). Advancing tracer-aided rainfall–runoff modelling: a review of progress, problems and unrealised potential. Hydrological Processes 29(25), 5227-5240

Bishop, M. A., Meyers, P. M., and P.F. McNeley. (2000). A method to estimate migrant shorebird numbers on the Copper River Delta, Alaska. Journal of Field Ornithology 71: 627-637.

Botter, G., Bertuzzo, E., & Rinaldo, A. (2010). Transport in the hydrologic response: Travel time distributions, soil moisture dynamics, and the old water paradox. Water Resources Research, 46(3).

Botter, G. (2012). Catchment mixing processes and travel time distributions. Water Resources Research, 48(5).

Brooks, J. R., Barnard, H. R., Coulombe, R., & McDonnell, J. J. (2010). Ecohydrologic separation of water between trees and streams in a Mediterranean climate. Nature Geoscience, 3(2), 100-104.

Butler, R. W., Williams, T. D., Warnock, N., and Bishop, M. A. (1997). Wind assistance: a requirement for migration of shorebirds? The Auk 114: 456-466.

Drever, M. C., Lemon, M. J., Butler, R. W., and Millikin, R. L. (2014). Monitoring populations of Western Sandpipers and Pacific Dunlins during northward migration on the Fraser River Delta, British Columbia, 1991–2013. Journal of Field Ornithology 85: 10-22.

Farmer, A. H., and F. Durbian. (2006). Estimating shorebird numbers at migration stopover sites. Condor 108, 792-807.

Freer, J., Beven, K., & Ambroise, B. (1996). Bayesian estimation of uncertainty in runoff prediction and the value of data: An application of the GLUE approach. Water Resources Research, 32(7), 2161-2173.

Frederiksen, M., A. D. Fox, J. Madsen, and K. Colhoun. (2001). Estimating the total number of birds using a staging site. Journal of Wildlife Management 65:282-289.

Harman, C. J. (2015). Time-variable transit time distributions and transport: Theory and application to storage-dependent transport of chloride in a watershed. Water Resources Research, 51(1), 1-30.

Hrachowitz, M., Savenije, H., Bogaard, T. A., Tetzlaff, D., & Soulsby, C. (2013). What can flux tracking teach us about water age distribution patterns and their temporal dynamics?. Hydrology and Earth System Sciences, 17, 533-564.

Hrachowitz, M., Fovet, O., Ruiz, L., & Savenije, H. (2015). Transit time distributions, legacy contamination and variability in biogeochemical $1/f^{\alpha}$ scaling: How are hydrological response dynamics linked to water quality at the catchment scale?. Hydrological Processes 29, 5241-5256.

Hrachowitz, M., Benettin, P., van Breukelen, B.M., Fovet, O., Howden, N.J.K., Ruiz, L., van der Velde, Y., & Wade, A.J. (2016). Transit times – how catchments store and release water. The link between hydrology and water quality at the catchment scale. WIREs Water 3, 629-657.

Iverson, G. C., Warnock, S. E., Butler, R. W., Bishop, M. A., & Warnock, N. (1996). Spring migration of western sandpipers along the Pacific coast of North America: a telemetry study. Condor 98, 10-21.

Iwamura, T., Possingham, H.P., Chadès, I., Minton, C., Murray, N.J., Rogers, D.I., Treml, E.A., & Fuller, R.A. (2013) Migratory connectivity magnifies the consequences of habitat loss from sea-level rise for shorebird populations. Proceedings of the Royal Society B: Biological Sciences, 280, 20130325.

McGuire, K. J., & McDonnell, J. J. (2006). A review and evaluation of catchment transit time modeling. Journal of Hydrology, 330(3), 543-563.

Myers, J.P., Morrison, R.I.G., Antas, P.Z., Harrington, B.A., Lovejoy, T.E., Sallaberry, M., Senner, S.E. & Tarak, A. (1987). Conservation strategy for migratory species. American Scientist, 75(1), 19-26.

Rappoldt, C., Kersten, M. & Smit, C. (1985). Errors in large-scale shorebird counts. Ardea, 73(1), 13-24.

Rinaldo, A., Beven, K. J., Bertuzzo, E., Nicotina, L., Davies, J., Fiori, A., Russo, D., & Botter, G. (2011). Catchment travel time distributions and water flow in soils. Water Resources Research, 47(7).

Rinaldo, A., Benettin, P., Harman, C. J., Hrachowitz, M., McGuire, K. J., Van der Velde, Y., Bertuzzo, E., & Botter, G. (2015). Storage selection functions: A coherent framework for quantifying how catchments store and release water and solutes. Water Resources Research, 51(6), 4840-4847.

Schaub, M., Pradel, R., Jenni, L., & Lebreton, J. D. (2001). Migrating birds stop over longer than usually thought: an improved capture-recapture analysis. Ecology, 82(3), 852-859.

Shao, J. (1993). Linear model selection by cross-validation. Journal of the American Statistical Association, 88(422), 486-494.

Taylor, C. M., Laughlin, A. J., & Hall, R. J. (2016). The response of migratory populations to phenological change: a Migratory Flow Network modelling approach. Journal of Animal Ecology 85, 648–659.

Van der Velde, Y., Torfs, P. J., Zee, S. E., & Uijlenhoet, R. (2012). Quantifying catchment-scale mixing and its effect on time-varying travel time distributions. Water Resources Research, 48(6).

Warnock, N., & Bishop, M. A. (1998). Spring stopover ecology of migrant Western Sandpipers. Condor 100, 456-467.

Warnock, N., Takekawa, J. Y., & Bishop, M. A. (2004). Migration and stopover strategies of individual Dunlin along the Pacific coast of North America. Canadian Journal of Zoology, 82: 1687-1697.

Warnock, N., M. A. Bishop, J. Y. Takekawa, & T. D. Williams. (2004) Pacific Flyway Shorebird Migration Program: Spring Western Sandpiper migration, Northern Baja California, Mexico to Alaska – Final Report 2004. PRBO Conservation Science, Stinson Beach, CA; Prince William Sound Science Center, Cordova, AK; U.S. Geological Survey, Vallejo, CA; and Simon Fraser University, Burnaby, BC, Canada.

Warnock, N., M. A. Bishop, J. Y. Takekawa, & T. D. Williams. (2006) Pacific Flyway Shorebird Migration Program: Spring Western Sandpiper migration, Pt. Mugu, California to Alaska. PRBO Conservation Science, Petaluma, CA; Prince William Sound Science Center, Cordova, AK; U.S. Geological Survey, Vallejo, CA; and Simon Fraser University, Burnaby, BC, Canada.

Ydenberg, R. C., Butler, R. W., Lank, D. B., Smith, B. D., & Ireland, J. (2004). Western sandpipers have altered migration tactics as peregrine falcon populations have recovered. Proceedings of the Royal Society of London, Series B: Biological Sciences, 271(1545): 1263-1269.

TABLES

Table 1. List of symbols and parameters used to estimate residence and transit times in the hydrological model for calculating length of stay of migrating birds.

Symbol	*Description*	*SI dimension symbol*
k	number of Monte Carlo realization	-
n	number of birds	-
n(t)	total number of birds present at time *t*	-
$n(t_R,t)$	number of birds with length of stay t_R that leave at time t	-
$p_{LOS}(t_R,t)$	distribution of length-of-stay for the birds leaving at time t	-
$p_R(t_R,t)$	distribution of ages t_R in storage (residence times) at time t	-
$p_T(t_R,t)$	distribution of ages t_R in outflux (transit times) at time t	-
$p_{T,m}$	mean transit time	T
$p_{T,m,k,\lambda}$	mean transit time of k^{th} model realization in λ^{th} year	T
t_i	time of first observation	T
$t_{i,n}$	time the n^{th} bird is first observed	T
$t_{o,n}$	time the n^{th} bird is last observed	T
t_R	residence time (length of stay)	T
B	beta function	-
J(t)	total influx at time t	LT^{-1}
$J_{min}(t)$	lower bound of total influx at time t	LT^{-1}
$J_{max}(t)$	upper bound of total influx at time t	LT^{-1}
$L(\alpha_{k,\lambda},\beta_{k,\lambda}\|LOS_{m,\lambda})$	likelihood measure for α and β of the k^{th} model realization in the λ^{th} year given $LOS_{m,\lambda}$	-
LOS	length-of-stay	T
LOS_n	length-of-stay for nth bird	T
LOS_m	mean length-of-stay	T
$LOS_{m,\lambda}$	mean length-of-stay in the λ^{th} year	T
O(t)	total outflux at time t	LT^{-1}
$O_{min}(t)$	lower bound of total outflux at time t	LT^{-1}
$O_{max}(t)$	upper bound of total influx at time t	LT^{-1}
$P_R(t_R,t)$	cumulative distribution of ages t_R in storage (residence times) at time t	-
S(t)	total storage volume at time t	L
$S(t_R,t)$	storage volumes of different residence times t_R at time t	L
α	shape parameter of beta distribution	-

Symbol	*Description*	*SI dimension symbol*
$\alpha_{k,\lambda}$	shape parameter of beta distribution for the k^{th} model realization in the λ^{th} year	-
β	shape parameter of beta distribution	-
$\beta_{k,\lambda}$	shape parameter of beta distribution for the k^{th} model realization in the λ^{th} year	-
λ	number of year	-
ω	Storage Age Selection (SAS) function	-

FIGURES

Figure 1:

Western Sandpiper migration dynamics at Sidney Island. Time series of (a) daily bird counts (or storage) S randomly sampled from the observed values of S ±25%, (b) daily bird arrival (or inflow) rates J, randomly sampled between J_{min} and J_{max} as obtained from equation (10), (c) daily bird departure (or outflow) rates O, randomly sampled between O_{min} and O_{max} as obtained from equation (11). The black lines in (a)-(c) indicate the time series associated with the $p_{T,m}$ that best describes the benchmark LOS_m for the respective year. Panel (d) shows the SAS function for each year, with values of α and β provide the 5/95th interval of their posterior distribution for each year. (e) Marginal transit time distributions p_T for each year (i.e. the outflow weighted averages of the individual daily transit time distributions). The black lines indicate the time series (a-c), the SAS function (d) and p_T (e) associated with the $p_{T,m}$ that best describe the benchmark LOS_m for the respective year. The grey shaded areas in (a)-(e) show the 5/95th uncertainty intervals of the respective variable, constructed from the weighted likelihood measures of each model realization (equation 17).

Figure 2:

Western Sandpiper migration dynamics at Roberts Bank. Time series of (a) daily bird counts (or storage) S randomly sampled from the observed values of S ±25%, (b) daily bird arrival (or inflow) rates J, randomly sampled between J_{min} and J_{max} as obtained from equation (10), (c) daily bird departure (or outflow) rates O, randomly sampled between O_{min} and O_{max} as obtained from equation (11). The black lines in (a)-(c) indicate the time series associated with the $p_{T,m}$ that best describes the benchmark LOS_m for the respective year. Panel (d) shows the SAS function for each year, with values of α and β provide the 5/95th interval of their posterior distribution for each year. (e) Marginal transit time distributions p_T for each year (i.e. the outflow weighted averages of the individual daily transit time distributions). The black lines indicate the time series (a-c),

the SAS function (d) and p_T (e) associated with the $p_{T,m}$ that best describe the benchmark LOS_m for the respective year. The grey shaded areas in (a)-(e) show the 5/95th uncertainty intervals of the respective variable, constructed from the weighted likelihood measures of each model realization (equation 17). The blue shaded areas in (a)-(e) indicate the 5/95th uncertainty intervals for years that were predicted. The different shades of grey and blue of the posterior distributions of the SAS functions (d) provide an anecdotal indication of which shapes of ω are more likely than others according to their relative cumulative weights in the posterior distribution. The blue shaded SAS function in (d) is the combined SAS function from the years 1992, 1994, 2002 and 2004, which is used as prior distribution for sampling the parameters α and β for the prediction of the remaining years.

Figure 3:

Dunlin migration dynamics at Roberts Bank. Time series of (a) daily bird counts (or storage) S randomly sampled from the observed values of S ±25%, (b) daily bird arrival (or inflow) rates J, randomly sampled between J_{min} and J_{max} as obtained from equation (10), (c) daily bird departure (or outflow) rates O, randomly sampled between O_{min} and O_{max} as obtained from equation (11). The black lines in (a)-(c) indicate the time series associated with the $p_{T,m}$ that best describes the benchmark LOS_m for the respective year. Panel (d) shows the SAS function for each year, with values of α and β provide the 5/95th interval of their posterior distribution for each year. (e) Marginal transit time distributions p_T for each year (i.e. the outflow weighted averages of the individual daily transit time distributions). The black lines indicate the time series (a-c), the SAS function (d) and p_T (e) associated with the $p_{T,m}$ that best describe the benchmark LOS_m for the respective year. The grey shaded areas in (a)-(e) show the 5/95th uncertainty intervals of the respective variable, constructed from the weighted likelihood measures of each model realization (equation 17). The blue shaded areas in (a)-(e) indicate the 5/95th uncertainty intervals for years that were predicted. The different shades of blue of the posterior distribution of the SAS function (d) provides an anecdotal indication of which

shapes of ω are more likely than others according to their relative cumulative weights in the posterior distribution. The posterior distribution of SAS function from 2001 (d) is used as prior distribution for sampling the parameters α and β for the prediction of the remaining years.

Figure 4:

Illustrations of hypothetical different sampling (or mixing) processes (after Harman, 2015). (a) a system characterized by a uniform SAS function, i.e. outflow is sampled from different ages in storage with equal probabilities (equivalent to the concept of a well-mixed reservoir and a beta distribution with $\alpha=\beta=1$). (b) a system that releases preferably younger ages in storage (beta distribution with $\alpha<1$, $\beta>1$). (c) a system that releases preferably older ages in storage (beta distribution with $\alpha>1$, $\beta<1$). The symbol S indicates age-ranked storage, J represents the input into the storage (e.g. arriving birds), O represents a flux released from storage (e.g. departing birds). Green shades indicate storage (i.e. bird counts), blue shades indicate in- or outflow, released from storage.

Figure 5:

Transit time distributions p_T and mean transit times $p_{T,m}$ for (a) Western Sandpiper at Sidney Island, (b) Western Sandpiper at Roberts Bank and (c) Dunlin at Roberts Bank. The red horizontal lines represent LOS_m estimates from radio-telemetry and mark-recapture approaches. Where available from literature (b,c), the standard deviations of LOS are shown as error bars to provide a sense of the distribution of LOS. The light grey triangle symbols represent the $p_{T,m}$ that comes closest to the benchmark LOS_m and the light grey error bars error bars represent the $5/95^{th}$ percentiles of the associated p_T. The dark grey circle symbols indicate the $p_{T,m}$ estimate derived from the average p_T of all feasible, likelihood weighted solutions. The dark grey error bars represent the associated averaged p_T. The light blue circles and error bars show estimates of $p_{T,m}$ and p_T, predicted for years without LOS_m estimates on basis of the combined posterior distributions from years with available LOS_m estimates. The insets show the distributions

of the actual mean transit times $p_{T,m}$ around their mean value (circle symbol; identical to circle symbols in large panels), derived from the individual likelihood weighted p_Ts of all feasible solutions. The diamond symbols in the insets represent estimates of upper bounds for $p_{T,m}$.

Figure 6:

Results of the cross validation analysis for (a) Western Sandpiper at Sidney Island, and (b) Western Sandpiper at Roberts Bank. The boxplots (horizontal line: median, box: interquartile range, whiskers: 5/95th interquantile range) represent the overall absolute deviations from the benchmark LOS_m estimates (dark gray boxplots) as well as deviations for the individual years (light grey), when in turn using the posterior distribution of the SAS function of each year as prior distribution to predict $p_{T,m}$ of the remaining years. The inset, in addition, provides the distributions of the actual $p_{T,m}$ (boxplot) predicted for each year compared to the benchmark LOS_m (red symbols).

1 Fig. 1

2

3 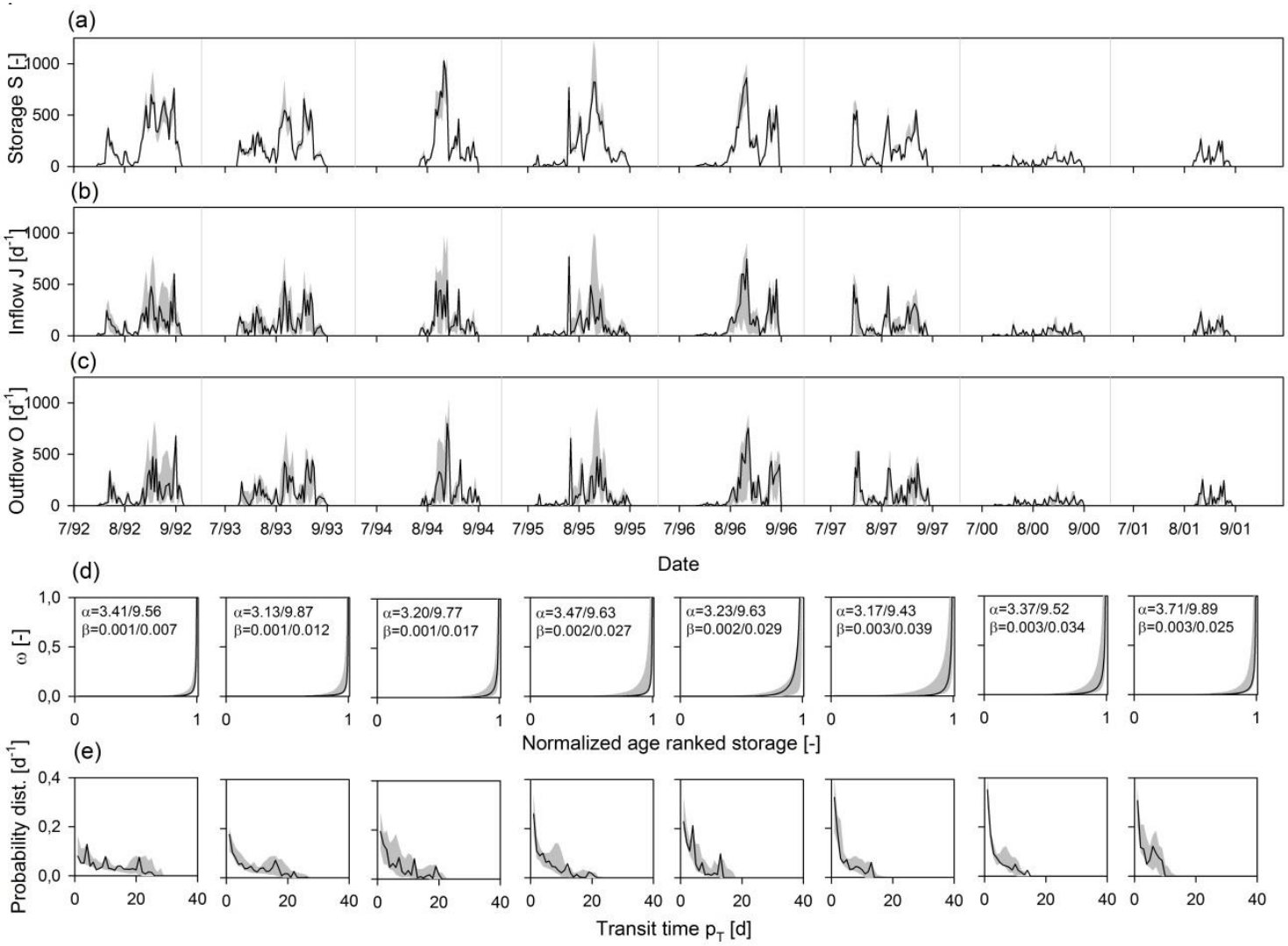
(a)
Storage S [-]
1000
500
0
(b)
Inflow J [d^{-1}]
(c)
Outflow O [d^{-1}]
7/92 8/92 9/92 7/93 8/93 9/93 7/94 8/94 9/94 7/95 8/95 9/95 7/96 8/96 9/96 7/97 8/97 9/97 7/00 8/00 9/00 7/01 8/01 9/01
Date
(d)
ω [-]
1,0
0,5
0,0
α=3.41/9.56 β=0.001/0.007
α=3.13/9.87 β=0.001/0.012
α=3.20/9.77 β=0.001/0.017
α=3.47/9.63 β=0.002/0.027
α=3.23/9.63 β=0.002/0.029
α=3.17/9.43 β=0.003/0.039
α=3.37/9.52 β=0.003/0.034
α=3.71/9.89 β=0.003/0.025
Normalized age ranked storage [-]
(e)
Probability dist. [d^{-1}]
0,4
0,2
0,0
0 20 40
Transit time p_T [d]

4 Fig. 2

5

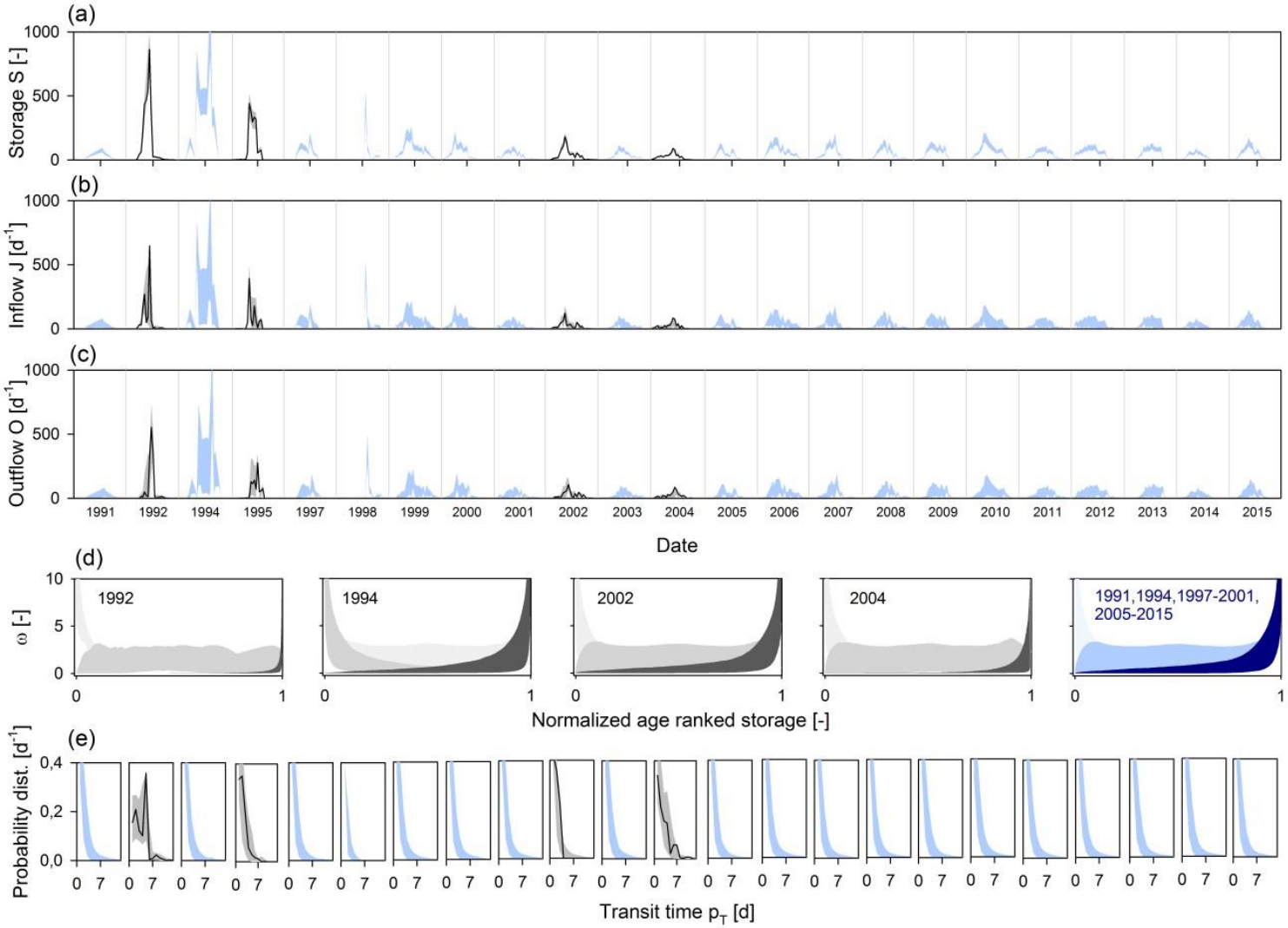
(a)
Storage S [-]
1000
500
0
(b)
Inflow J [d^{-1}]
(c)
Outflow O [d^{-1}]
1991 1992 1994 1995 1997 1998 1999 2000 2001 2002 2003 2004 2005 2006 2007 2008 2009 2010 2011 2012 2013 2014 2015
Date
(d)
ω [-]
10
5
1992
1994
2002
2004
1991,1994,1997-2001,
2005-2015
Normalized age ranked storage [-]
(e)
Probability dist. [d^{-1}]
0,4
0,2
0,0
Transit time p_T [d]

Fig. 3

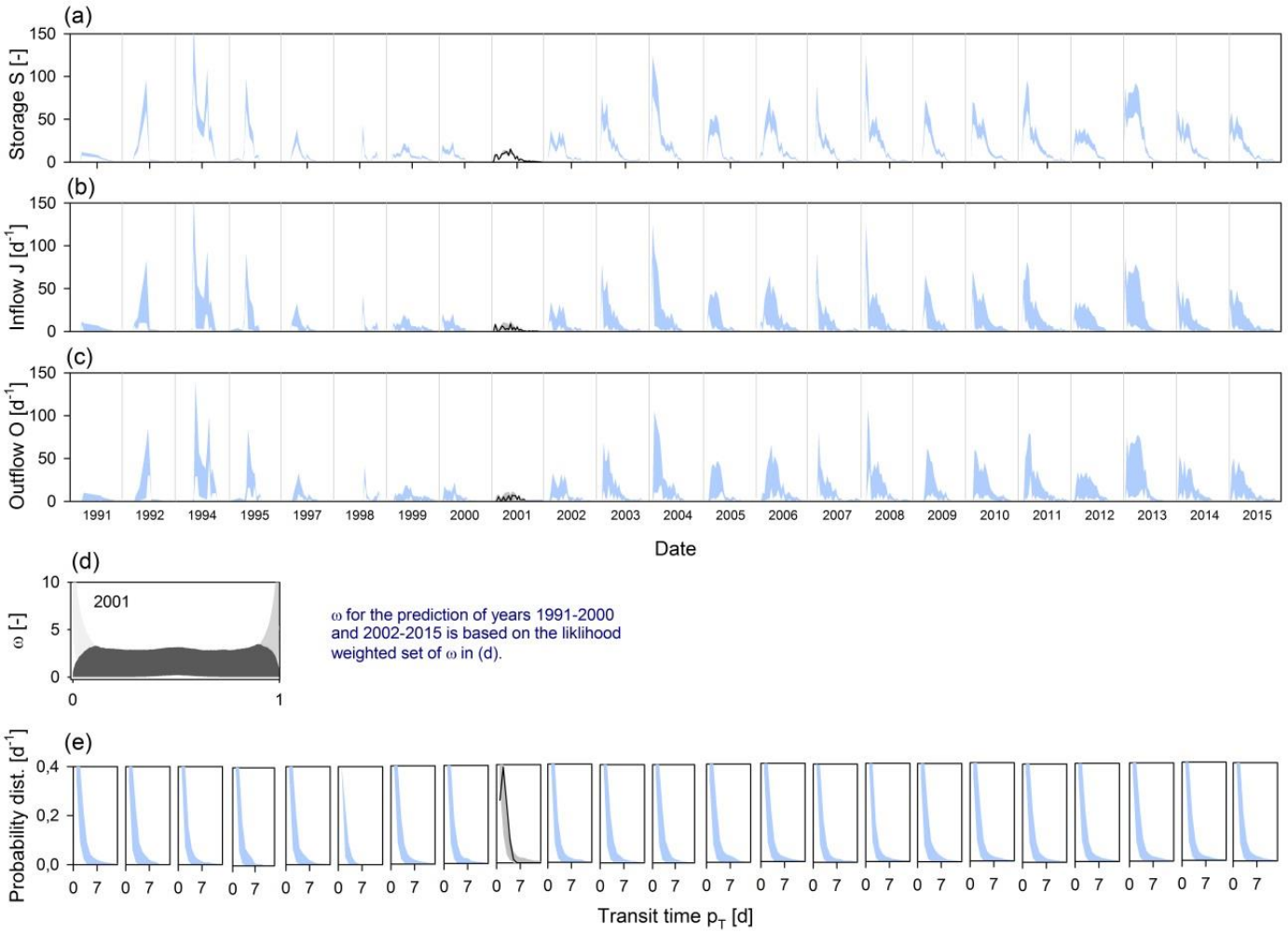
(a)
Storage S [-]
150
100
50
0
(b)
Inflow J [d^{-1}]
(c)
Outflow O [d^{-1}]
1991 1992 1994 1995 1997 1998 1999 2000 2001 2002 2003 2004 2005 2006 2007 2008 2009 2010 2011 2012 2013 2014 2015
Date
(d)
ω [-]
10
5
0
2001
0
1
ω for the prediction of years 1991-2000 and 2002-2015 is based on the liklihood weighted set of ω in (d).
(e)
Probability dist. [d^{-1}]
0,4
0,2
0,0
0 7
Transit time p_T [d]

Fig.4

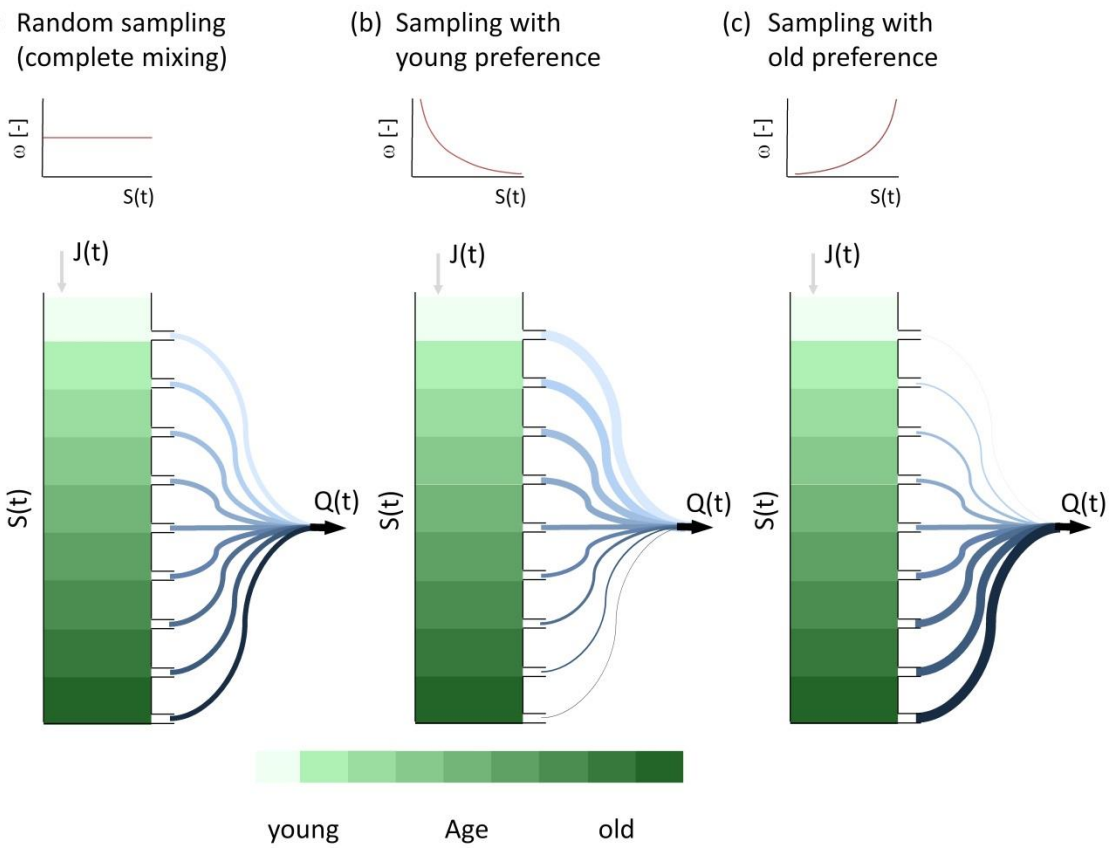
(a) Random sampling
(complete mixing)
(b) Sampling with
young preference
(c) Sampling with
old preference
ω [-]
S(t)
J(t)
Q(t)
young
Age
old

Fig.5

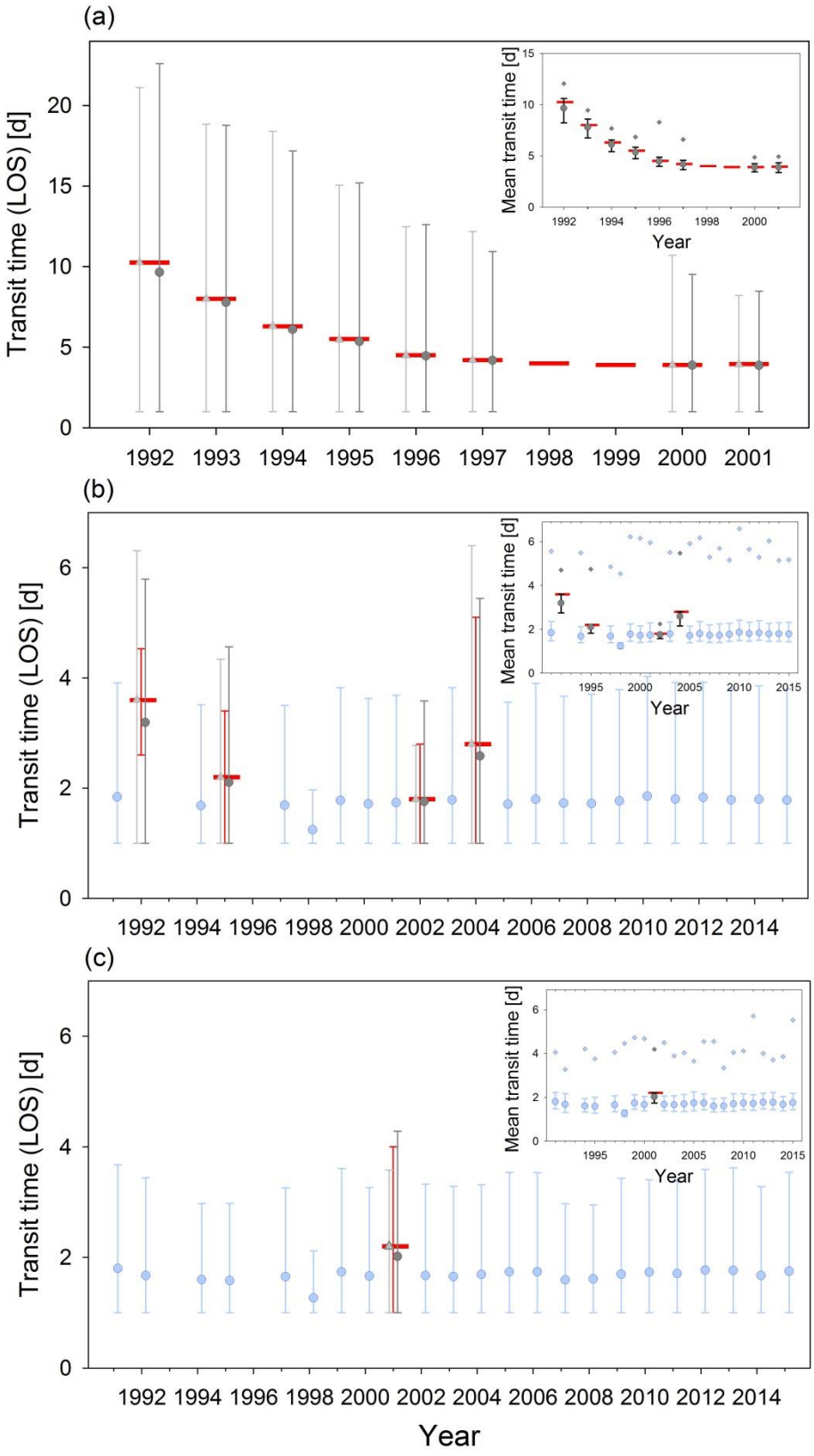
(a)
Transit time (LOS) [d]
Mean transit time [d]
Year
(b)
Transit time (LOS) [d]
Mean transit time [d]
Year
(c)
Transit time (LOS) [d]
Mean transit time [d]
Year
Year

Fig.6

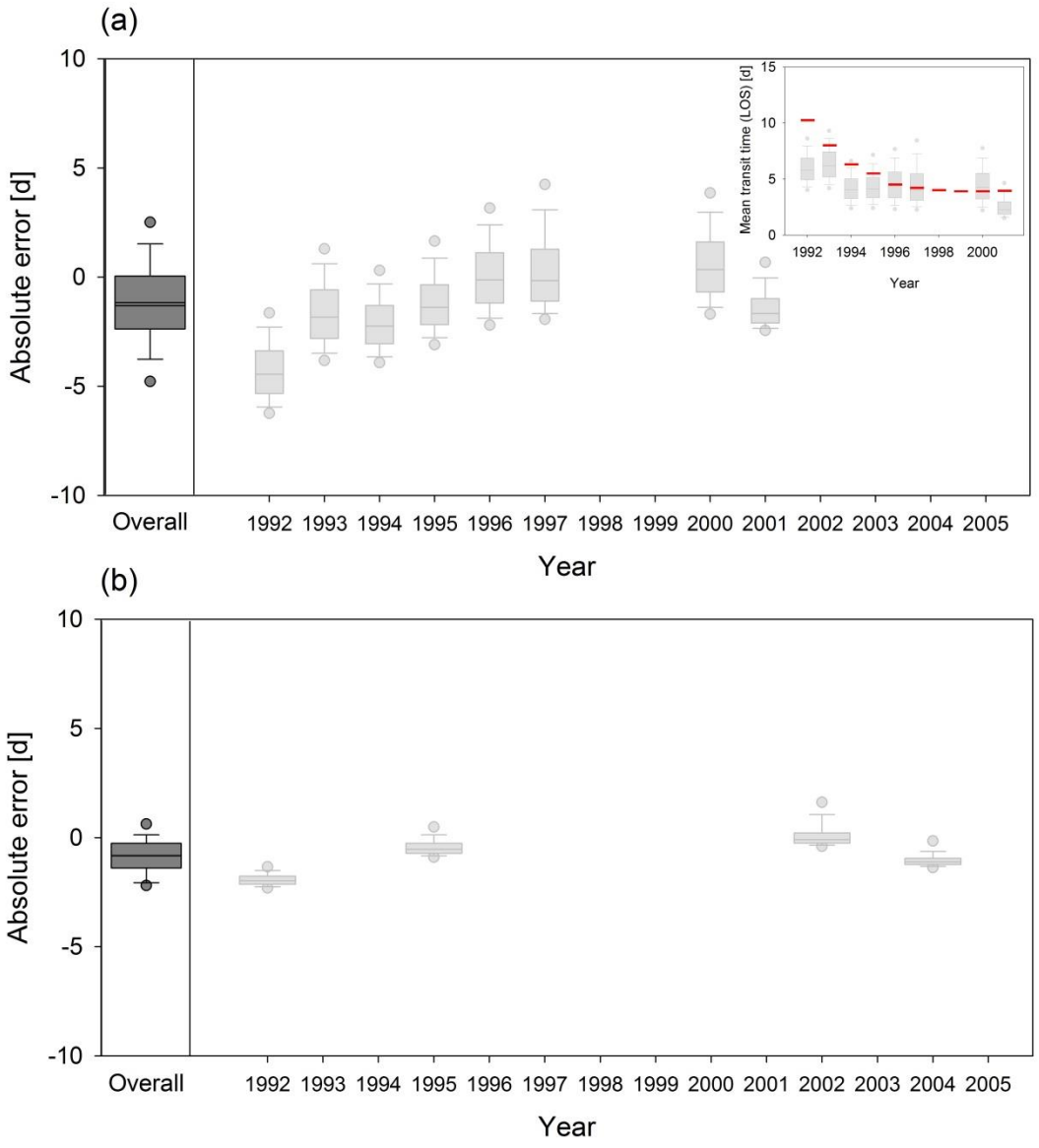
(a)
Absolute error [d]
10
5
0
-5
-10
Overall
1992 1993 1994 1995 1996 1997 1998 1999 2000 2001 2002 2003 2004 2005
Year
Mean transit time (LOS) [d]
15
10
5
0
1992 1994 1996 1998 2000
Year
(b)
Absolute error [d]
10
5
0
-5
-10
Overall
1992 1993 1994 1995 1996 1997 1998 1999 2000 2001 2002 2003 2004 2005
Year